Journal of ELECTRICAL ENGINEERING, VOL. 56, NO. 9-10, 2005, 258–264

LOAD CHARACTERISTICS AND CONTROL SYSTEM BEHAVIOURAL MODELLING UNDER OPTIMAL TRAJECTORY CONTROL OF SERIES RESONANT DC/DC CONVERTERS

Nikolay Bankov * — **Tsvetana Grigorova** **

The paper presents behavioural modelling of the control system of series resonant DC/DC converters operated above the resonant frequency under "optimal trajectory control" technique. This method predicts the fastest response possible with minimum energy surge in the resonant tank. The steady-state equations described the converter operation above the resonant frequency as a function of the diode trajectory radius and corresponding normalized load characteristics are proposed. They allow evaluating the behaviour of the considered converter when the load is changed strongly during the operation process. Simulation and experimental results are given.

K e y w o r d s: resonant DC/DC converters, control system, optimal trajectory control, behavioural modelling

1 INTRODUCTION

Several control methods of series resonant DC/DC converters are widely discussed and compared in recent years [1–6]. Due to the presence of a resonant circuit with its fast transient response, the control of resonant converters is considerably more complex than of PWM converters [1]. The tank processes fast dynamics and exchanges large amounts of pulsating energy with the source and with the load in each half-cycle of converter operation. The advantages of the examined optimal trajectory control method over the existing methods are a reduced stress on the reactive and power semiconductor switching elements of the circuit and a faster response in the case of large variations of circuit operating conditions without affecting the global stability of the system [7].

Emphasis in this paper is on obtaining steady state equations describing the DC/DC resonant converter operation above the resonant frequency as a function of the diode trajectory radius and corresponding normalized load characteristics, which are useful to design such a converter. The control system is described using Analog Behavioural Modelling (ABM) feature provided in OrCad PSpice [8].

2 ANALYSIS AND LOAD CHARACTERISTICS OF THE RESONANT DC/DC CONVERTER

Figure 1 shows the proposed DC/DC converter. The converter is operated above the resonant frequency.

Analysis is made under the following assumptions: the converter elements are ideal; the effect of snubber capacitors and the ripples of input and output voltages are neglected; the output capacitor is sufficiently large such that the output voltage U_0 remains constant through a switching cycle.

The following common symbols are used:
$\omega_0 = 1/\sqrt{LC}$ — angular resonant frequency; $Z_0 = \sqrt{L/C}$ — characteristic impedance; ω — switching fre-

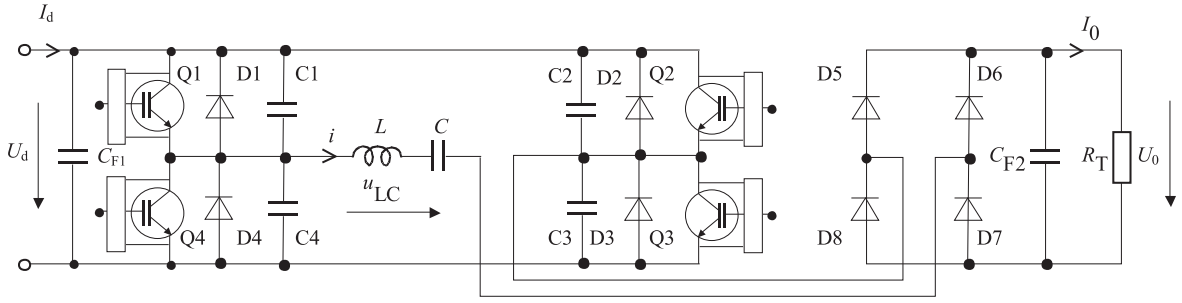

Fig. 1. Full-bridge DC/DC resonant converter.

* University of Food Technologies, Department of Electronics, 26 Maritza Blvd., 4002 Plovdiv, Bulgaria, nikolay_bankov@yahoo.com

** Technical University of Sofia, Branch Plovdiv, Department of Electronics, 61 Sankt Petersburg Blvd., 4000 Plovdiv, Bulgaria, c_grigorova@abv.bg

ISSN 1335-3632

quency; $i'(0) = I'_{L0}$, $u'(0) = U'_{C0}$ — normalized initial values of the resonant link current and voltage across series capacitor for each stage of the converter operation; $\Theta_Q = \omega_0 t_Q$ — transistors conduction angle; $\Theta_D = \omega_0 t_D$ — diodes conduction angle; $U'_0 = \frac{U_0}{gU_d}$ — voltage ratio, where g is topology constant ($g = 0.5$ for half-bridge topologies and $g = 1$ for full-bridge topologies).

For unifying purposes all units are presented as relative ones: the voltages to the supply voltage U_d; the currents to the current $I = U_d/Z_0$; the input power to the power $P = U'_d/Z_0$.

Under optimal trajectory control of series resonant DC/DC converters operating above the resonant frequency, the converter is analysed with the use of the state plane. Figure 2 shows one steady-state trajectory above the resonant frequency.

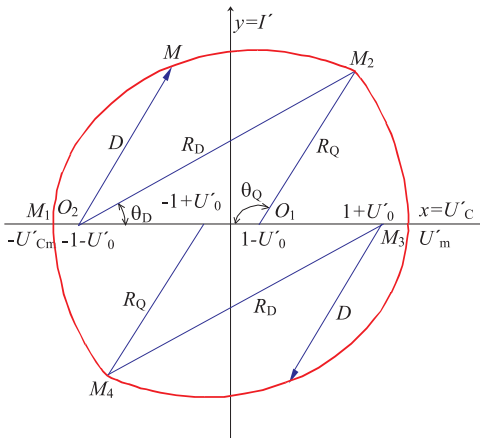

Fig. 2. SRC steady-state trajectory above resonant frequency.

The expressions of current $i(\omega_0 t)$ and voltage $u_C(\omega_0 t)$ in each sequence are:

$$i(\omega_0 t) = \frac{u_{LC} - u_C(0)}{Z_0} \sin \omega_0 t + i(0) \cos \omega_0 t\,, \tag{1}$$

$$u_c(\omega_0 t) = u_{LC} - [u_{LC} - u_C(0)] \cos \omega_0 t + i(0) Z_0 \sin \omega_0 t\,. \tag{2}$$

In the $(u_C/U_d\,,\, i\sqrt{L/C}/I)$ state plane [8], the trajectory described by the operating point is an arc of a circle with its centre at the point of coordinates $(u_{LC}, 0)$ and drawn from the representative point of the initial conditions $(u'_C(0)\,,\, i'(0)\sqrt{L/C})$.

The four centres are given by $\{Q1/Q3\colon (1 - U'_0, 0)\}$, $\{D1/D3\colon (1 + U'_0, 0)\}$, $\{Q2/Q4\colon (-1 + U'_0, 0)\}$ and $\{D2/D4\colon (-1 - U'_0, 0)\}$. The optimal trajectory control above the resonant frequency utilizes the desired diode trajectory as the control low.

In the first half period, distance D (Fig. 2) of the state of the system from the centre of trajectory located at $\{(-1 - U'_0), 0\}$ is monitored. When this distance is smaller than radius value R_D, as set by the control system, transistors $Q1/Q3$ are turned on (segment M_1M_2). When distance D becomes equal to control input R_D at M_2, transistors are turned off and diodes $D2/D4$ are switched on (segment M_2M_3). At point M_3 the diodes switch off, as resonant current reverses. Then transistors $Q2/Q4$ are turned on (segment M_3M_4). Distance D is once again monitored, this time as measured from the $D1/D3$ trajectory centre $\{(1 + U'_0, 0)\}$.

From the triangle $O_1O_2M_2$ (Fig. 2) the following equations for the diodes trajectory radius R_D and transistors trajectory radius R_Q are obtained

$$R_D = 1 + U'_0 + U'_{Cm}\,, \tag{3}$$

$$R_Q = 1 - U'_0 + U'_{Cm} = R_D - 2U'_0\,. \tag{4}$$

As can be calculated in [7], radius R_D is evaluated

$$R_D = U'_0 + \sqrt{1 + (1 - U'^2_0) \tan^2\Big(\frac{\Theta_Q + \Theta_D}{2}\Big)}. \tag{5}$$

For the transistors and diodes conduction angles it can be written

$$\Theta_Q + \Theta_D = \frac{\pi}{\omega/\omega_0} = 2 \arctan \sqrt{\frac{(R_D - U'_0)^2 - 1}{1 - U'^2_0}}. \tag{6}$$

The peak capacitor voltage in the relevant units is given by

$$U'_{Cm} = R_D - 1 - U'_0\,. \tag{7}$$

The normalized average transistors current becomes

$$I'_{Q_{AV}} = \frac{(1 - U'^2_0)(1 - \cos\Theta_Q)}{2(U'_0 + \cos\Theta_Q)(\Theta_Q + \Theta_D)} = \frac{(1 + U'_0)(R_D - 1 - U'_0)}{4 \arctan \sqrt{\frac{(R_D - U'_0)^2 - 1}{1 - U'^2_0}}}. \tag{8}$$

The normalized average diodes current can be expressed as follows

$$I'_{D_{AV}} = \frac{(1 - U'^2_0)(1 - \cos\Theta_Q)}{2(U'_0 + \cos\Theta_Q)(\Theta_Q + \Theta_D)} = \frac{(1 - U'_0)(R_D - 1 - U'_0)}{4 \arctan \sqrt{\frac{(R_D - U'_0)^2 - 1}{1 - U'^2_0}}}. \tag{9}$$

The normalized average load current is given by

$$I'_0 = 2\big(I'_{Q_{AV}} + I'_{D_{AV}}\big) = \frac{(R_D - 1 - U'_0)}{\arctan \sqrt{\frac{(R_D - U'_0)^2 - 1}{1 - U'^2_0}}}. \tag{10}$$

The average input current in relative units is

$$I'_d = 2\big(I'_{Q_{AV}} - I'_{D_{AV}}\big) = \frac{U'_0(R_D - 1 - U'_0)}{\arctan \sqrt{\frac{(R_D - U'_0)^2 - 1}{1 - U'^2_0}}}. \tag{11}$$

For the normalized transistors peak current we can obtain the equations

$$I'_{Qm} = R_Q = R_D - 2U'_0\,, \qquad \Theta_Q \geq \pi/2\,, \tag{12}$$

$$I'_{Qm} = \big(R_d - 2U'_0\big) \sin\Theta_Q\,, \qquad \Theta_Q < \pi/2\,. \tag{13}$$

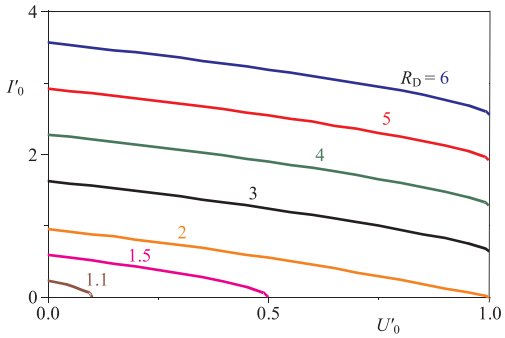

Fig. 3. Output characteristics for several values of R_D.

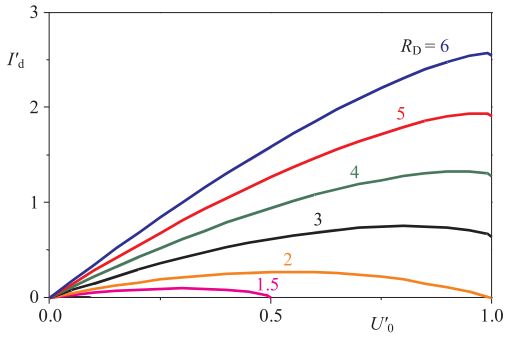

Fig. 4. Normalized input current I'_d

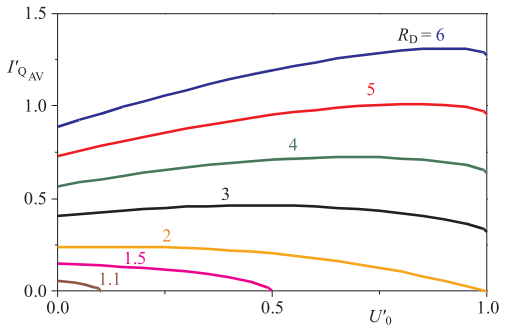

Fig. 5. Normalized transistors average current $I'_{Q_{AV}}$ versus U'_0.

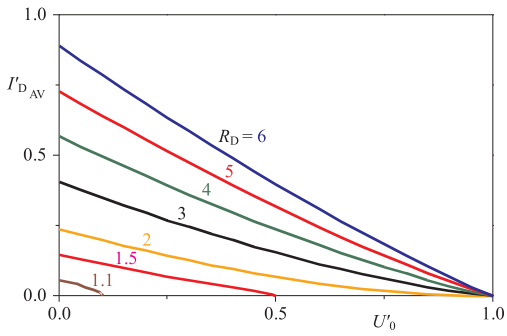

Fig. 6. Normalized diodes average current $I'_{D_{AV}}$ versus U'_0.

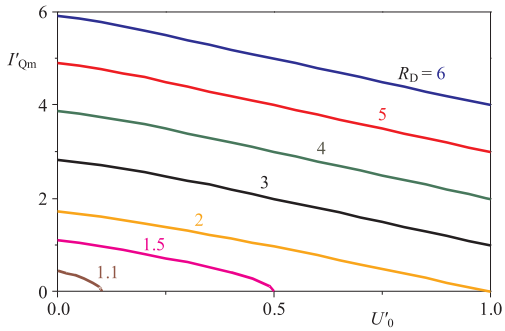

Fig. 7. Normalized transistors peak current versus U'_0.

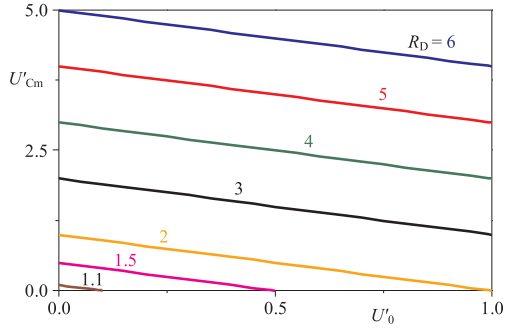

Fig. 8. Normalized peak capacitor voltage U'_{Cm} versus U'_0.

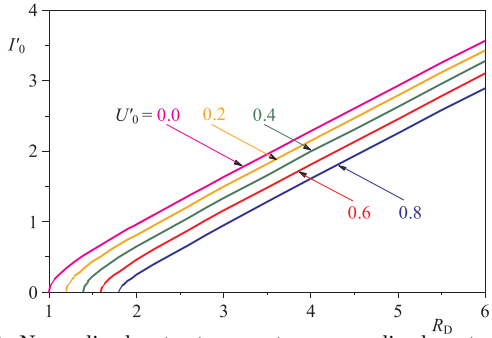

Fig. 9. Normalized output current vs normalized control input.

The transistors and diodes conduction angles are

$$\Theta_Q = \arccos\frac{1 - U'_0 - U'_0U'_{Cm}}{1 - U'_0 + U'_{Cm}} = \arccos\frac{1 - U'_0R_D - U'^2_0}{R_D - 2U'_0} \qquad (14)$$

and

$$\Theta_Q = \arccos\frac{1 + U'_0 + U'_0U'_{Cm}}{1 + U'_0 + U'_{Cm}} = \arccos\frac{1 + U'_0R_D - U'^2_0}{R_D}. \qquad (15)$$

As a proof of the analysis it is possible to define the optimal control low which allows transient processes with large amplitude, at same time a stable converter operation (transistors and resonant tank) are ensured. Variable D is defined (Fig. 2) as the distance between the representative point of the system and the commutating centre of the reference trajectories:

$$D = \sqrt{i'^2 + [u'_C + \operatorname{sign} i'(1 + U'_0)]^2}. \qquad (16)$$

Transistors turn-off is realized when $D = R_D$. If $D > R_D$ transistors are turned on while $D = R_D$ or $\Theta_Q = \pi$.

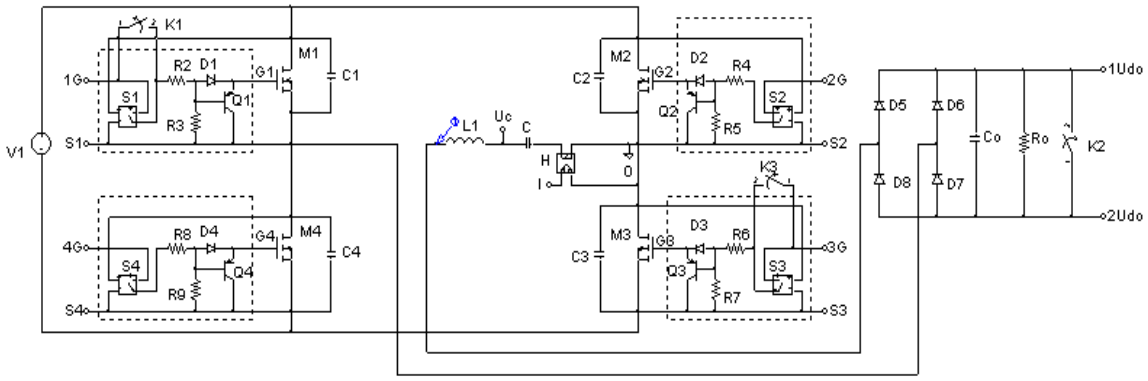

Fig. 10. The simulation full-bridge resonant DC/DC converter.

Practically, to ensure transistors soft switching conditions (ZVS) it is necessary

$$\Theta_Q < \pi \quad \text{and} \quad I' > I'_{\min}\,. \tag{17}$$

On solving equations (3)– (13), one can draw a family of inverter load characteristics. Those are the relationships of the converter main variables as a function of the voltage ratio U'_0 and radii R_D. The following relations can be of great interest: the converter output current $I'_0(U'_0, R_D)$, the input current $I'_d(U'_0, R_D)$, the transistors average current $I'_{Q_{AV}}(U'_0, R_D)$ and the freewheeling diodes average current $I'_{D_{AV}}(U'_0, R_D)$, the peak transistors current $I'_{Qm}(U'_0, R_D)$, the peak capacitor voltage $U'_{Cm}(U'_0, R_D)$. Figures 3–8 show corresponding graphs by $R_D = 1.1;\ 1.5;\ 2 \div 6$ in relative units.

The relationships $I'(U_0, R_D)$ (Fig. 3) represent the converter output characteristics. The converter can be considered as a current source, stable at short-circuit mode. Its operation near no-load running mode is limited from the transistors soft switching conditions (ZVS) [9].

The relationships $I'(R_D, U'_0)$ (Fig. 9) represent dc characteristics which are useful in determining the control range for require output variation. Another important concern is whether by limiting the maximum value of the control input a current-limited output can be obtained. This is important in determining the need of additional overcurrent protection circuit.

The study of the characteristics shown in Figs. 3–9 reveals that they can be used to calculate the circuits elements of the SRC — for example, the transistors average current I'_{Qav} can be calculated from Fig. 5 for a selected values of U'_0 and R_D.

3 BEHAVIORAL MODELLING OF THE OPTIMAL TRAJECTORY CONTROL SYSTEM

The control system is described using Analog Behavioural Modelling (ABM). The ABM feature provided in OrCad PSPICE allows flexible descriptions of electronic components in terms of the transfer function or lookup table. In other words, a mathematical relationship is used to model a circuit segment so the segment need not be designed component by component. Moreover, the combination of significant calculation efficiency with adequate component's modelling is achieved [8]. Figure 10 shows the simulation resonant DC/DC converter.

Individual transistor control circuits are introduced. These circuits feed the gate drive pulses of the corresponding transistor, if at the individual circuit input has drive signal and the transistor drain-source voltage is practically zero. This control method can be better understood by looking at the waveforms shown in Figure 11.

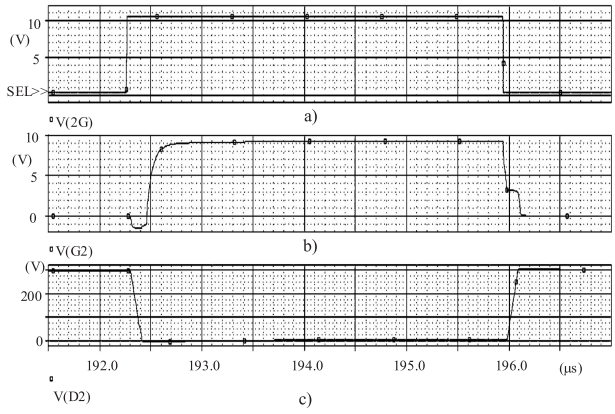

Fig. 11. Individual control circuit — a) input driving signals and b) output driving signals, c) the transistor M2 drain-source voltage.

The drive pulse appears on the transistor M2 individual circuit input (Fig. 11a) immediately after the transistor M3 is turned off, because the two transistors are operated with the voltages, dephased at 180°. The drain-source voltage of the M2 (Fig. 11c) becomes practically zero, after the snubber capacitors C2 and C3 are recharged. In this way, only by zero voltage of the transistor M2 (ZVS), the gate drive pulse (Fig. 11b) is ensured.

The proposed control system (CS) is shown in Fig. 12 and in Fig. 13 — the waveforms, which explain the system operation.

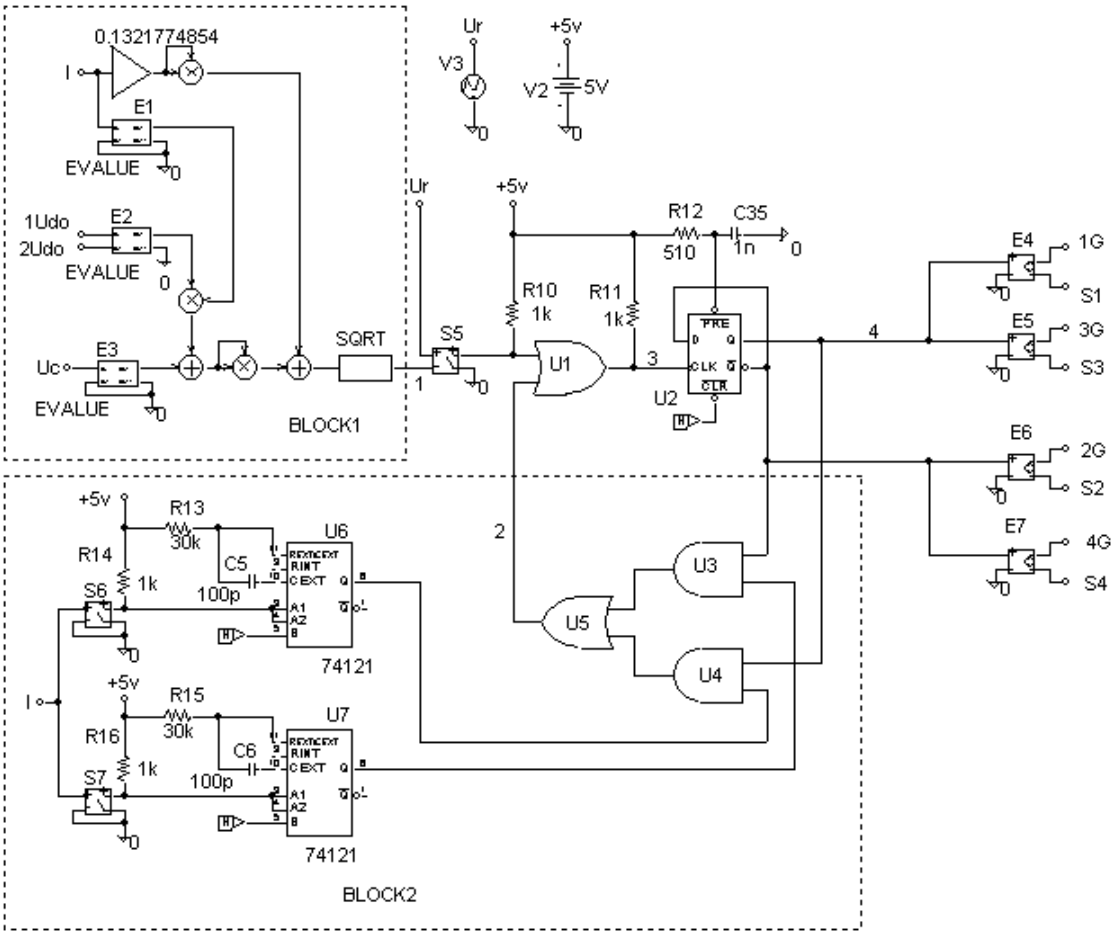

Fig. 12. Converter control system behavioural modelling.

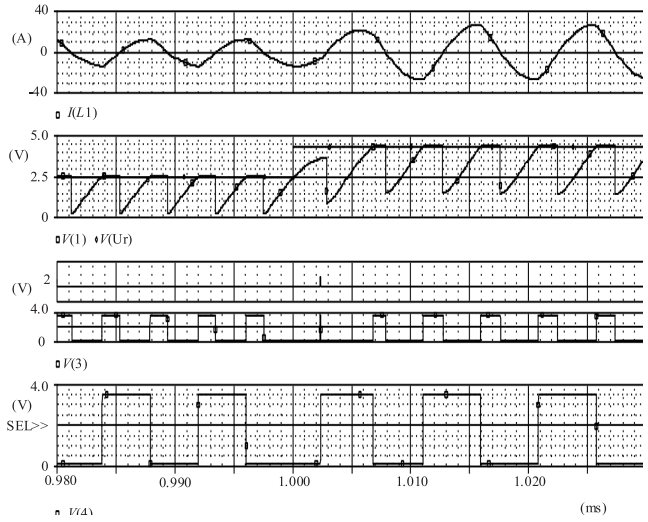

Fig. 13. Control system main waveforms.

From the instantaneous values of i, u_C, U_0 and U_d, the control circuits computes the variable D at every instant as given by eq. (16) BLOCK1.

The dependent current control voltage source (CCVS) H senses the current trough the resonant tank. The signals for voltages U_0 and u_C are fed to the dependent voltage sources of EVALUE type (E2 and E3). The output of E1 (EVALUE) is the logical signal whose state ($+1$ or -1) is determined by the sign i'. The dependent voltage source E1 realizes function:

$$\text{SGN(V(\%IN+,\%IN-))} \tag{18}$$

in the EXPRESSION field of the EVALUE element.

The received value of D (v (1) in Fig. 12) is compared with control signal Ur.

The voltage controlled switches S6, S7, one-shot multivibrators 74121 and logical elements U3, U4, U5 ensure soft switching condition eq. (17) (BLOCK2).

The shaped pulses are fed to the flip-flop trigger U2. The pulse distributor U2 forms two channels of the control pulses, dephased at 180°. The dependent voltage control voltage sources (VCVS) E4 ÷ E7, provide the required power, amplitudes and galvanic separation of the control signals.

As noted in [1,9], the maximum rate at which the tank energy can change in half a cycle is limited. Thus the system takes more than a half-cycle to reach the target trajectory. Figure 14 shows the PSpice simulation results of the system response to large changes in control input.

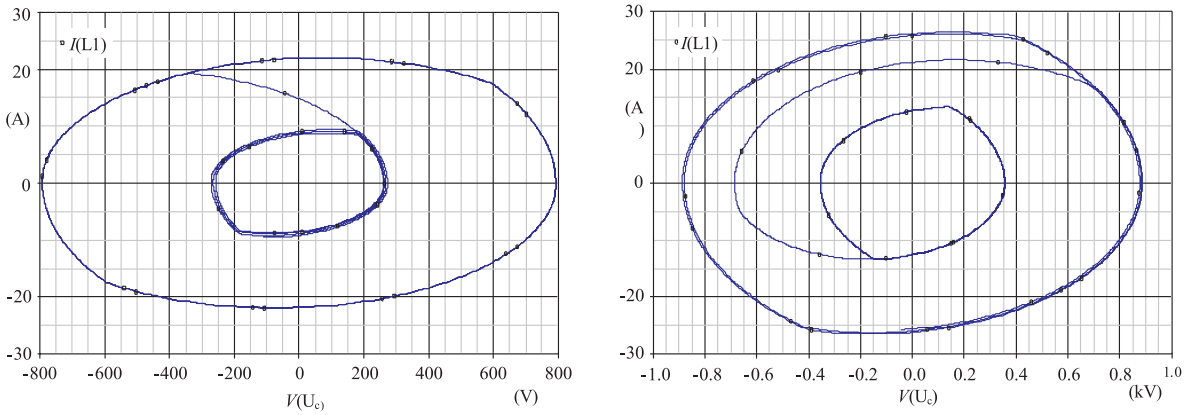

Fig. 14. Response of optimal trajectory control for a) Control decrease $R_{D1} = 4.3 \rightarrow R_{D2} = 2.5$ $(t = 1980 \div 2030\,\mu\text{s})$, b) Control increase $R_{D1} = 2.5 \rightarrow R_{D2} = 4.3$ $(t = 980 \div 1030\,\mu\text{s})$

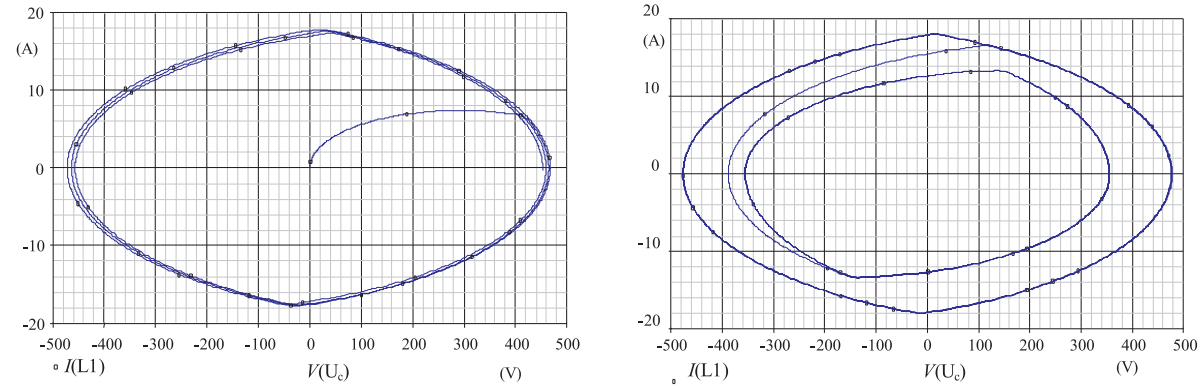

Fig. 15. Transient under a) Converter start-up $R_D = 2.5$ $(t = 0 \div 30\,\mu\text{s})$, b) Load short circuit $R_D = 2.5$ $(t = 2980 \div 3030\,\mu\text{s})$

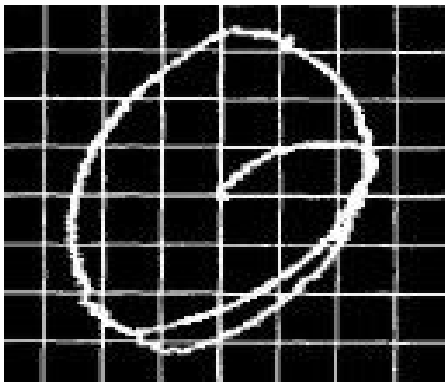

Fig. 16. Start-up of the converter — x: $u_C(200\,\text{V/div})$ and y: $I_{L1}(5\,\text{A/div})$.

In Fig. 14a, when control input decrease, the tank energy is reduced by a series of successive diode conductions.

Likewise in Fig. 14b, when control input increase, the tank energy is built up a series of successive transistor conductions. Thus by utilizing the desired diode trajectory itself as the control low, the new steady state can be reached. In both cases, the system reaches the new equilibrium trajectory in the minimum possible time limited only by the intrinsic properties of the resonant converter.

Figure 15a shows PSpice simulation results of the system response at converter start-up. The performance of the method under short-circuit is also remarkable as shown in Fig. 15b. Within a short time, the system abruptly reaches another equilibrium trajectory at energy level only slightly greater than the earlier one. Thus optimal trajectory control fully exploits the potential of a converter to respond quickly to the demands of control and load.

5 EXPERIMENTAL RESULTS

The computer simulation and experimental results of the resonant DC/DC converter are given by the following conditions: power supply $U_1 = 300$ V; switching frequency $f = 125$ kHz; output power $P = 3$ kW; and resonant link elements $L = 72.577\,\mu$H and $C = 46.157$ nF. During the experiment snubbers' value is 1 nF.

Figure 16 shows converter start-up optimal trajectory. Very good agreement between simulation and experimental results can be seen.

4 CONCLUSIONS

In this paper we obtained steady-state equations in optimal trajectory control, described DC/DC resonant converter operation above the resonant frequency as a function of the diode trajectory radius and corresponding normalized load characteristics. They allow evaluating the behaviour of the considered converter when the load is changed strongly during the operation process. The control system is described using ABM feature provided in OrCad PSpice.

The resonant tank energy is fully controlled with the tank energy, current and voltage, all staying well within bounds under all circumstances, including a short circuit across the converter output. The control automatically selects the optimum sequence of device condition under dynamic conditions. Very good agreement between simulation and experimental results can be seen.

The converters operated under this control technique are more suitable for electric arc welding devices, X-ray devices, lasers power supply *etc*, where for the supply source, characteristics of the current source are required.

References

[1] ORUGANTI, R.—LEE, F. C.: Resonant Power Processor: Part II — Methods of control,, Proc. IEEE-IAS'84 Ann. Meet., pp. 868–878 , 1984.

[2] CHERON, Y.: La commutation douce dans la conversion statique de l'energie electrique, Technique et Documentation — Lavoisier, 1989.

[3] SIVAKUMAR, S.—NATARAJAN, K.—SHARAF, A. M.: Optimal Trajectory Control of Series Resonant Converter using Modified Capacitor Voltage Control Technique, Proc. IEEE–PESC'91 Ann. Meet., Cambridge-Boston, pp. 752–759, June 1991.

[4] NATARAJAN, K.—SIVAKUMAR, S.: Optimal Trajectory Control of Constant Frequency Series Rsonant Converter, 24th Annual IEEE Power Electronics Specialists Conference PESC '93, pp. 215–221, June 1993.

[5] ROSSETTO, L.: A Simple Control Technique for Series Resonant Converter, IEEE Trans. on Power Electronics **11** No. 4 (July 1996), 554–560.

[6] KUTKUT, N. H.—LEE, C. Q.—BATARSEH, I.: A Generalized Program for Extracting the Control Characteristics of Resonant Converters via the State-Plane Diagram, IEEE Trans. on Power Electronics **13** No. 1 (January 1998), 58–66.

[7] SENDANYOYE, V.—AL HADDAD, K.—RAJAGOPALAN, V.: Optimal Trajectory Control Strategy for Improved Dynamic Response of Series Resonant Converter, Proc. IEEE-IAS'90 Ann. Meet., Seattle, WA, pp. 1236–1242, (October 1990).

[8] OrCAD PSpice A/D User's Guide, OrCAD Inc., USA, 1999.

[9] AL-HADDAD, K.—CHERON, Y.—FOCH, H.—RAJAGOPALAN, V.: Static and Dynamic Analysis of a Series Resonant Converter Operating above its Resonant Frequency, SATECH'86 Proceedings, Boston, pp. 55-68, 1986.

Received 30 May 2005

Nikolay Dimitrov Bankov was born in 1957 in Plovdiv, Bulgaria. He received the MS degree in electrical engineering from the Technical University Sofia in 1983. In 1998 he received his PhD in electrical converters. He is Assoc. Prof. in the University of Food Technologies, Department of Electronics. His research interests are in the fields of applied electronics, power electronics, control techniques and digital simulation.

Tsvetana Grigorova Grigorova was born in 1968 in Plovdiv, Bulgaria. She received the MS degree in electronics and automation from the Technical University Sofia in 1991. In 2000 she received her PhD in electrical converters. Since 1992 till now she has been Assist. Prof. in Technical University of Sofia, Branch Plovdiv, Department of Electronics. Her current interests include the development of high-frequency resonant converters and their control, behavioural modelling using PSpice. Dr. Grigorova is a member of IEEE Power Electronics Society.